Inertial Response and Inertia Emulation in DFIG and PMSG Wind Turbines: Emulating Inertia from a Supercapacitor-based Energy Storage System

Javier Sacristán
Dept. of Electrical, Electronic and Communications Engineering
Public University of Navarre (UPNA), Campus de Arrosadía
31006 Pamplona, Spain
javier.sacristan@unavarra.es

Naiara Goñi
Dept. of Electrical, Electronic and Communications Engineering
Public University of Navarre (UPNA), Campus de Arrosadía
31006 Pamplona, Spain
goni.111213@e.unavarra.es

Alberto Berrueta
Institute of Smart Cities
Dept. of Electrical, Electronic and Communications Engineering
Public University of Navarre (UPNA), Campus de Arrosadía
31006 Pamplona, Spain
alberto.berrueta@unavarra.es

Jesús López
Institute of Smart Cities
Dept. of Electrical, Electronic and Communications Engineering
Public University of Navarre (UPNA), Campus de Arrosadía
31006 Pamplona, Spain
jesus.lopez@unavarra.es

José Luis Rodríguez
Dept. of Onshore Electrical Module
Siemens Gamesa Renewable Energy
31621 Sarriguren, Spain
JOSE.L.RODRIGUEZ@siemensgamesa.com

Alfredo Ursúa
Institute of Smart Cities
Dept. of Electrical, Electronic and Communications Engineering
Public University of Navarre (UPNA), Campus de Arrosadía
31006 Pamplona, Spain
alfredo.ursua@unavarra.es

Pablo Sanchis
Institute of Smart Cities
Dept. of Electrical, Electronic and Communications Engineering
Public University of Navarre (UPNA), Campus de Arrosadía
31006 Pamplona, Spain
pablo.sanchis@unavarra.es

***Abstract*— The increasing wind power penetration in electrical power systems results in a reduction of operative conventional power plants. These plants include synchronous generators directly connected to the grid. Facing a change in grid frequency, these generators inherently respond by varying their stored kinetic energy and their output power, which contributes to grid stability. Such a response is known as inertial response. Wind turbines (WTs) are mostly based on Doubly-Fed Induction Generator (DFIG) or Permanent Magnet Synchronous Generator (PMSG) machines. Their power electronics interface decouples the electromechanical behaviour of the generator from the power grid, making their inertial response null or insignificant. Therefore, in order not to weaken the frequency response of the power system, WTs must be able to react to frequency variations by changing their output power, i.e., emulating an inertial response. Common techniques for inertia emulation in WTs rely on pitch control and stored kinetic energy variation. This contribution proposes a strategy (applicable for both DFIG and PMSG) which uses the energy stored in a supercapacitor connected to the back-to-back converter DC link to emulate the inertial response. Its performance is compared by simulation with aforementioned common techniques, showing ability to remove certain limitations.**

Keywords*— wind; frequency; kinetic energy; inertia; inertial response; inertia emulation; synthetic inertia; DFIG; PMSG; supercapacitor; energy storage; DC link.

I. Introduction

In an electrical power system, an imbalance between generated and consumed power causes a frequency variation. To ensure stability and safe operation of the power system, the Transmission System Operator (TSO) controls the frequency to remain within a strict range. To do so, conventional generation plants automatically adjust their generated power to compensate for any imbalance, thereby avoiding large frequency excursions. This grid service is known as primary regulation. Any power controller used to provide primary regulation has inherent delays, so a change in system frequency is inevitable in the first moments after the imbalance.

A synchronous generator directly connected to the grid rotates at a speed defined by the grid frequency, i.e., it is coupled to the grid. Therefore, a frequency variation causes a change in its rotational speed, thereby modifying the kinetic energy stored in the rotating mass. For instance, facing a frequency drop caused by increased demand, the synchronous generator decelerates, releasing a fraction of its stored kinetic energy and injecting it into the grid. This inherent response contributes to the grid stability, compensating the initial increase in demand and attenuating the Rate of Change of Frequency (RoCoF). The variation of its stored kinetic energy caused by a change in frequency is known as inertial response (IR), which is discussed in detail in [1].

Wind turbines (WTs) are not based on synchronous generators coupled to the grid. Most of them are based on Doubly-Fed Induction Generator (DFIG) or Permanent Magnet Synchronous Generator (PMSG) machines. These generation topologies include electronic power converters. Regarding PMSG machines, the electronic power converter completely decouples the electric generator and its electromechanical behaviour from the power grid. This implies that they do not experience a natural variation of their stored kinetic energy due to a frequency change, i.e., they do not contribute with an IR. In contrast, a DFIG is sensitive to frequency events, but the implemented control loops, which are responsible for operating the WT at the Maximum Power Point (MPP), make the IR insignificant [2], [3].

Power systems are continuously installing more Wind Power Plants (WPPs), replacing conventional power plants (most of them based on synchronous generators coupled to the grid). Therefore, system inertia is continually declining, implying that the frequency of these systems is increasingly sensitive to generation-demand imbalances. This has led to different TSOs limiting wind power penetration [4]. Therefore, in order to keep the increasing wind power penetration without weakening the frequency response, WTs

This work has been supported by Siemens Gamesa Renewable Energy, by the Spanish State Research Agency (AEI/ 10.13039/501100011033) under grants PID2019-111262RB-I00 and PID2019-110956RB-I00, and by the Public University of Navarra under project ReBMS PJUPNA1904.

978-1-6654-3613-7/21/$31.00 ©2021 IEEE

need to be able to react to frequency variations by changing their output power. This ability is known as artificial, emulated, simulated or synthetic inertia [5]. Everything indicates that, over time, most TSOs will demand this type of performance from WPPs, so the study of how to emulate an IR in WTs is, and will be, a key work line for WT manufacturers.

Currently, the most common technique for inertia emulation (IE) in WTs (in both PMSG and DFIG) consists of including a series of controllers that, by modifying pitch angle setpoint or allowing WT stored kinetic energy variations, achieve an output power change while facing a frequency event [6]. One of the drawbacks of this IE technique is that relying on the variation of the stored kinetic energy to emulate the IR leads to a variation of the turbine rotational speed. Therefore, WT is forced to leave the MPP, losing the ability to capture the maximum available wind power and leading to a reduction in the Annual Energy Production (AEP).

In this contribution, an IE technique for both PMSG and DFIG that keeps the turbine at the MPP, with no variation of its rotational speed, is proposed. The proposed system includes a supercapacitor (SC) connected to the DC link of the back-to-back power converter. The energy stored in this SC is used to emulate the IR. The DC link voltage setpoint is used as the control variable to achieve this IR, thereby determining the SC power during any frequency event. In addition to the advantage already mentioned (always operating at MPP), this technique proves competence to eliminate specific limitations shown by the conventional technique (based on pitch control and stored kinetic energy variation).

The remaining of this contribution is organised as follows. Section II is devoted to discussing the IR of PMSG and DFIG WTs. Section III analyses the conventional techniques for emulating inertia in PMSG and DFIG WTs. The proposed IE strategy is presented in Section IV, where its advantages over conventional technique are also discussed. Simulation results are presented in Section V to compare the performance of both strategies. Finally, Section VI introduces the conclusions of this contribution.

II. Inertial Response of PMSG and DFIG Wind Turbines

This section discusses the IR of a PMSG and a DFIG in their standard configurations, i.e., without being modified to provide them with the ability to emulate inertia.

A PMSG, DFIG or any other WT topology will exhibit an IR to a change in grid frequency if such a frequency change causes a variation in the machine's rotational speed (Ω), i.e., in its stored kinetic energy. If the mechanical torque provided by the WT rotor (T_m) is considered to remain constant, the machine will vary its speed if the electromagnetic torque (T_{em}) is sensitive to changes in frequency. Therefore, a WT will contribute with an IR if T_{em} is affected by frequency variations [2].

Regarding PMSG, the generator's stator is connected to the grid via a back-to-back converter (AC/DC-DC/AC). The intermediate DC link included in the converter ensures that the grid frequency is completely decoupled from the frequency at generator's stator windings. Therefore, T_{em} is not sensitive to frequency variations, which allows to conclude that a PMSG in its standard configuration does not contribute with an IR.

In contrast, in a DFIG, the generator's stator is directly connected to the grid. To be able to draw conclusions about its IR, the relationship between T_{em} and the grid frequency in this WT topology is further analysed. The expression of DFIG T_{em} in a synchronous rotating reference frame oriented to stator magnetic field is shown in (1):

$$T_{em} = -\frac{3}{2} p \frac{L_m}{L_s} \psi_s i_{qr} \tag{1}$$

where p is the number of the generator's pole pairs, L_m is its magnetizing inductance, L_s is the stator inductance (defined as the sum of stator leakage inductance and magnetizing inductance), ψ_s is the stator flux and i_{qr} is the rotor quadrature current (referred to stator) [7].

At the same time, neglecting the small voltage drop in stator resistance, ψ_s can be expressed as shown in (2):

$$\psi_s \approx \frac{v_s}{\omega_s} \approx \frac{v_s}{2\pi f} \tag{2}$$

where v_s is stator voltage, ω_s is the synchronous electrical speed and f is the grid frequency [7]. These expressions show that T_{em} is sensitive to grid frequency changes.

A DFIG incorporates a control structure to get it to operate in the MPP, known as Maximum Power Point Tracking (MPPT). There are different strategies for implementing this control. Fig. 1 shows the generalised control schemes of two of the most widely implemented strategies [8].

From (1) and (2), facing a frequency drop, initially ψ_s rises, causing an increase in T_{em}. Since T_m remains constant, the machine decelerates, releasing a fraction of its stored kinetic energy and injecting it into the grid, leading to an increase in output power (P_{out}).

In case the DFIG incorporates an MPPT strategy as presented in Fig. 1(a), rotational speed setpoint (Ω^*) slowly tracks changes in P_{out} with a lowpass filter time constant of several seconds [9]. Therefore, during the first instants of the frequency event, Ω^* can be considered constant despite the increase in P_{out}. The initial machine deceleration sets Ω lower than Ω^*. The controller $G_\Omega(s)$ reacts to the speed error by decreasing the value of the electromagnetic torque setpoint (T^*_{em}), trying to reduce the generator's braking torque that would suppose a rise in Ω. In a DFIG, the Rotor Side Converter (RSC) incorporates a control that ensures that T_{em} follows T^*_{em}, cancelling the IR.

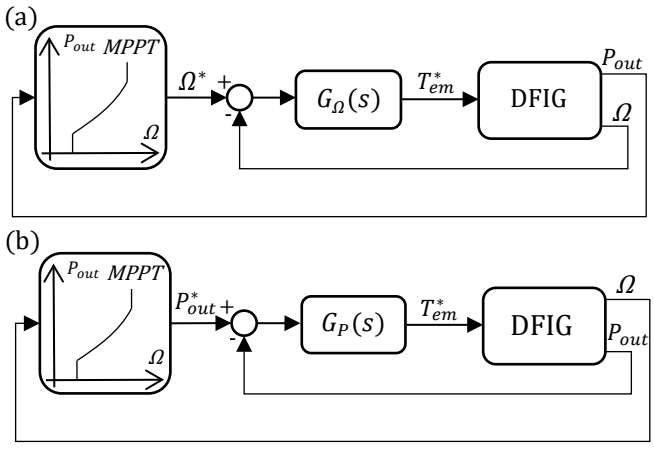

Fig. 1. Generalised control block diagrams of two of the most widely implemented MPPT strategies for DFIG: (a) based on rotational speed closed-loop control; (b) based on output power closed-loop control.

Analogously to the previous case, if the implemented MPPT strategy obeys the scheme shown in Fig. 1(b), output power reference (P^*_{out}) can be considered constant during the first instants of the frequency event despite the reduction in Ω. Due to the initial increase in P_{out}, it becomes higher than P^*_{out}. The controller $G_P(s)$ reacts to this power error by decreasing the value of T^*_{em}, in search of a machine acceleration. By doing so, the desired P_{out} reduction would be achieved, since a fraction of the mechanical power provided by the WT rotor would be destined to accelerate the machine rather than being transformed into electrical power. As in the previous case, the RSC ensures that T_{em} follows T^*_{em}, annulling the IR.

Therefore, the magnitude and duration of the IR is determined by the speed of $G_\Omega(s)$ and $G_P(s)$ in reacting to rotational speed and power errors, respectively, by modifying T^*_{em}. These controllers are tuned to act with a speed which only allows slight deviations of Ω around Ω^*. This controller tuning leads to variations in captured mechanical power being transformed into variations in stored kinetic energy. All rotating masses act as a buffer to mechanical power variations. Then, electrical power fluctuations (also known as flicker) are smoothed out [3], [9]. Since only small deviations in Ω are allowed, the IR is greatly limited, almost insignificant.

III. Conventional Inertia Emulation in PMSG and DFIG Wind Turbines

The previous section allows to conclude that a PMSG IR to a frequency event is null and that a DFIG contributes with an almost insignificant IR. Therefore, in order to increase wind power penetration in an electrical power system without worsening its frequency response, WTs need to be able to reply to a change in frequency by varying their output power, i.e., emulating an IR.

Currently, the most common technique for IE in WTs (in both DFIG and PMSG) consists of the following: the grid frequency is measured in turbine terminals and filtered by means of a low-pass filter to reject measurement noise; a series of controllers receive as an input the value of the RoCoF or the frequency deviation from nominal value; depending on this input, they modify the electromagnetic torque, active power or rotational speed setpoint of the electronic converters and pitch angle control loops. This allows an active output power variation when frequency changes, i.e., emulating an IR. In case of a decrease in frequency, if WT is operating with rated output power, where the pitch angle is different from optimal in order to limit captured power, the IR is achieved by decreasing the pitch angle, capturing that extra power that is needed. However, if WT is operating with less than rated output power, with optimal pitch angle, the IR is achieved by extracting a fraction of its stored kinetic energy. This leads to a machine deceleration, causing it to leave the MPP. For the turbine to regain its original speed and re-operate in the MPP, the period of increased output power is followed by a period of decreased output power, as the kinetic energy extracted from rotating masses needs to be recovered from mechanical captured power. This period is known as recovery process [6], [10].

A state-of-the-art review of the different types of IE controllers is provided in [6]. It classifies them into three main categories: Natural Inertial Control (NIC), Step-wise Inertial Control (SIC) and Virtual Inertial Control (VIC). In NIC, WT active output power is changed in proportion to RoCoF, frequency deviation or both. In SIC, upon detecting an under-frequency event, a constant (or variable, depending on the specific strategy chosen) over-production amount of power is delivered to the grid for several seconds. In VIC, when a frequency deviation is detected, output power is rapidly regulated by switching the turbine operating point from the MPPT curve (with optimal power curve coefficient k_{opt}) to a VIC power tracking curve (with a variable curve coefficient k_{VIC} that is function of frequency deviation).

In case of implementing NIC or SIC strategies, when the WT exits frequency regulation and starts the recovery process, additional power falls directly to zero, and output active power decreases instantaneously. This power shortage leads to an undesired Secondary Frequency Drop (SFD) after the frequency Nadir [11]. With VIC, during the recovery process, the VIC curve coefficient is continuously changed till reaching k_{opt}, due to the continuous variation of the frequency deviation. Then, the recovery is a smooth process without sharp output power drops, which avoids the SFD [6].

Fig. 2 shows the generalised control scheme of a rotational speed closed-loop MPPT that includes a NIC based on both RoCoF and frequency deviation from nominal value. This could be indistinctly implemented in a PMSG or in a DFIG. Facing a decrease in frequency, the IE controller reacts by adding an additional T_{em} setpoint (ΔT^*_{em}) in order to control the deceleration of the machine and the release of stored kinetic energy to output the desired power increase (ΔP). The structure incorporates two deadbands, so as not to act on continuous small perturbations in frequency that occur during normal operation of the power system. Furthermore, it incorporates a high-pass filter for not responding to steady-state frequency errors. It is important to remark that, to allow the machine deceleration during the frequency event, it is necessary to decrease the speed of the controller $G_\Omega(s)$ (or of $G_P(s)$ in case of opting for an output power closed-loop MPPT, as the one shown in Fig. 1(b)) [9].

There are different criteria for determining the value of constants $k_{df/dt}$ and $k_{\Delta f}$. Setting $k_{df/dt}$=2H (where H is the WT inertia constant, expressed in seconds) and $k_{\Delta f}$=0, the expression of ΔP (in p.u.) is shown in (3):

$$\Delta P = -2Hf\frac{df}{dt} \tag{3}$$

where f is the grid frequency, in p.u. With this selection of constants $k_{df/dt}$ and $k_{\Delta f}$, the WT tries to mimic the IR of a synchronous generator directly connected to the grid [12].

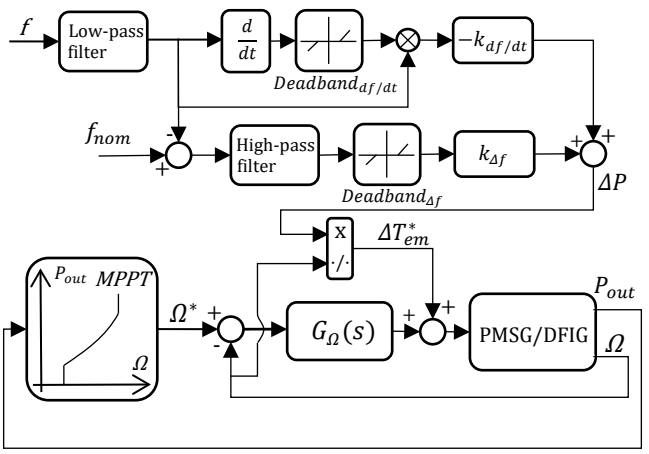

Fig. 2. Generalised control scheme of a rotational speed closed-loop MPPT that includes a NIC based on both RoCoF and frequency deviation (for PMSG or DFIG).

The optimal value of $k_{df/dt}$ and $k_{\Delta f}$ for achieving highest RoCoF attenuation and maximum Nadir frequency depends on the power system to which the WTs are connected [13]. Types of power plants and wind power penetration have significant influence. Different power system compositions were analysed and the optimal $k_{df/dt}$ value was always zero (or close to zero). This means that, by setting $k_{df/dt}$ to zero, it is possible to obtain an optimal IR without calculating *df/dt*, which is always a noise amplifying process and could result in undesired oscillations in P_{out}. The IE strategy reduces to a fast droop control strategy, also known as Fast Frequency Response (FFR). It also states that, if WTs opt for this parameter setting, it is feasible to improve the system's frequency response when replacing conventional generators with WTs.

IV. Proposed Inertia Emulation Strategy for PMSG and DFIG Wind Turbines

The IE strategy proposed in this contribution includes a SC directly connected to the DC link of the back-to-back power converter. The energy stored in this SC is the only energy source for the IR emulation, without resorting to stored kinetic energy or blade pitching. SC operation is controlled by regulating the DC link voltage setpoint. This strategy could be implemented in both PMSG and DFIG WTs.

Fig. 3 shows the control scheme of the proposed technique. Facing a decrease in frequency, the IE controller reacts by setting the DC link voltage setpoint (V^*_{DC}) below rated DC link voltage (V_{DCnom}). In both DFIG and PMSG, the Grid Side Converter (GSC) incorporates a control that ensures that the DC link voltage (V_{DC}) follows its setpoint. Then, a fraction of SC stored energy is released and injected into the grid, emulating the IR. The magnitude of the additional output power is controlled by modifying k_{DC}. The structure incorporates a low-pass filter to reject measurement noise; a high-pass filter for not responding to steady-state frequency errors; and a deadband for not acting on continuous small perturbations in frequency that occur during normal operation of the system.

An IE strategy for PMSG that simultaneously extracts stored kinetic energy from the rotating masses and stored energy from the DC link capacitor has been proposed [14]. As no additional Energy Storage System (ESS) is connected to the DC link, its contribution is greatly limited. Alternatively, other authors propose two strategies for DFIG that rely on both WT rotational kinetic energy and energy from a SC coupled to the DC link [15]. In the first one, both energy sources are used simultaneously. In the second one, firstly employs SC energy and then rotational kinetic energy via a cascading control, the latter being the source of greater weight when generating the response. Techniques for emulating inertia in a DFIG by connecting a SC in the DC link via an additional DC/DC converter, that regulates the SC operation, have been also proposed [11], [16]. Unlike all the referenced similar works, with the strategy proposed in this contribution, IE is achieved exclusively from the stored energy in a SC directly connected to the DC link (without an additional DC/DC converter).

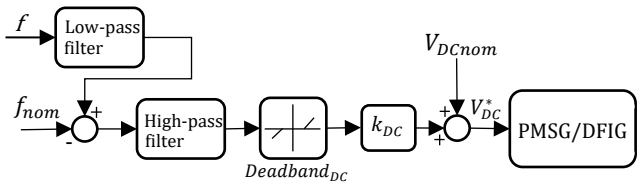

Fig. 3. Generalised control scheme of the proposed IE technique

The proposed technique in this contribution has a number of important advantages over conventional techniques (based on pitch control and stored kinetic energy variation) that are listed below:

- Relying on variation of stored kinetic energy to emulate the response, the WT changes its speed, so is forced to leave the MPP, losing the ability to capture the maximum available wind power. With the proposed technique, the WT keeps operating at the MPP, since it does not imply speed variations. This leads to an AEP improvement.
- Ω must remain within a range Ω_{min}-Ω_{max}. Illustrative ranges are 0.5-1.2 p.u. for PMSG and 0.7-1.2 p.u. for DFIG [6]. If an underfrequency event occurs when wind speed is lower than its cut-in speed (WT is stopped), equal or slightly higher than its cut-in speed (WT is rotating at Ω_{min} or close to it) or higher than its cut-out speed (WT is stopped), the available IR is null or very limited with conventional technique implementation. The proposed technique has maximum capacity to emulate inertia regardless wind speed, even when the WT is stopped.
- Relying on kinetic energy variations, facing an underfrequency event, the increased T_{em} leads to a speed decline. Turbine deceleration tends to reduce aerodynamic lift, thereby reducing T_m and aggravating the speed decline. This positive feedback tends to push the blades towards aerodynamic stall, which must be avoided. IE is limited for low Ω to provide a margin above the stall [9]. The proposed strategy solves this problem, as T_{em} is not increased.
- With conventional technique, to alleviate mechanical stresses on the drive train caused by abrupt Ω changes that suppose a reduction of WT's lifetime, the rate of change of output power is limited. It should not exceed 0.45 p.u./s according to several manufacturers [6]. With the proposed strategy, output power does not have this limitation.
- As the WT keeps operating at the MPP during the frequency event, the proposed strategy avoids the SFD.
- With the conventional technique, during the speed recovery process associated to an underfrequency event, WT output power is lower than the power it was injecting into the grid before the frequency event, as it is not operating in the MPP and a fraction of mechanical captured power is being destined to accelerate the machine. The primary regulation service contributes with additional power support to compensate this generation loss. It is crucial that the speed recovery process takes place just after the event, as turbines need to re-operate in the MPP as soon as possible to minimize the aforementioned generation loss. The higher demand on the primary regulation service delays the frequency recovery to the nominal value [17]. With the proposed strategy, it is not essential that the recovery process (associated to the SC charging phase) happens just after the event, as turbines keep operating in the MPP. Recovery could start once the frequency has reached nominal value. This means that, after the period of increased output power, WT output power could be equal to the power it was injecting into the grid before the event, without overloading the primary regulation service and avoiding a delay in frequency recovery.
- Because of slow nature of mechanical pitch angle controller system [16], emulating inertia by modifying pitch angle setpoint could delay the response upon detecting a frequency event. The SC fast dynamics avoid this delay.

- To achieve the same additional output power, the amount of kinetic energy that the WT rotating masses have to release is higher than the energy that the SC has to discharge. The reason is that mechanical losses in the drive train added to electrical losses in the generator and back-to-back converter (in both RSC and GSC) are greater than SC discharge losses added to GSC electrical losses. Therefore, the proposed strategy has a higher efficiency.

All these advantages make it clear that the proposed IE strategy outperforms conventional IE approaches, but it requires the inclusion of an additional component (the SC), which increases the initial investment of the solution. The SC market is experiencing a remarkable expansion, accompanied by intensive research and development aimed at reducing cost [18]. SC decreasing price makes the proposed IE strategy increasingly competitive.

V. Simulation Results and Discussion

This section aims to compare by simulation the IR of a DFIG in its standard configuration (i.e., without any IE technique implemented), including a conventional IE strategy and incorporating the IE technique proposed in this contribution, facing the same frequency event.

The frequency event selected for the comparison is shown in Fig. 4(a), which corresponds to a simulation (carried out by ENTSO-E [19]) that illustrates the evolution of the Continental European Power System frequency in case of a 3 GW generation loss (which represents the dimensioning incident for the primary regulation service control) in a particular scenario. In this scenario, of the 405 GW total load, 107 GW are supplied by wind power (26.42%), so represents a situation with high wind power penetration. The initial RoCoF is – 0.075 Hz/s and the Nadir frequency is 49.825 Hz. After primary regulation service actuation, frequency reaches its stationary value of 49.92 Hz. The secondary regulation service does not react to raise the frequency to its nominal value of 50 Hz.

Simulations were carried out in MATLAB/SIMULINK, using a 1.6-MW DFIG model, which has an H of 5.04 s [20]. The DFIG includes a rotational speed closed-loop MPPT, as the one shown in Fig. 1(a). All simulations are carried out with a constant wind speed of 12 m/s. Under this wind speed conditions, the WT rotates at Ω_{max} (1.2 p.u.) and outputs less than rated power (0.79 p.u.) before the frequency event.

For studying the response of the DFIG with conventional IE, a representative IE strategy of several commercial solutions ([9], [21]) is implemented. These solutions opt for a FFR technique. Then, following Fig. 2 scheme, $k_{df/dt}$ is set to zero. $k_{\Delta f}$ is tuned to respond to this particular frequency event with a maximum additional output power of 0.05 p.u. (5% of rated power). In addition, in these commercial solutions, $Deadband_{\Delta f}$ is adjusted to react only to large frequency excursions, those for which IR is relevant to ensure grid stability. In this case, $Deadband_{\Delta f}$ is fixed to ±0.0025 p.u., as proposed in [9].

For the implementation of the proposed strategy (shown in Fig. 3), k_{DC} is tuned to offer the same maximum additional output power as in the previous case (0.05 p.u.). To be able to respond with this extra power and, at the same time, keep the DC link voltage within its operating limits, a 5.16 F SC is included. To improve the frequency response of the power system to all kind of events and not only to those that compromise the grid stability, this proposal opts for adjusting $Deadband_{DC}$ with tighter ranges (null for this simulation).

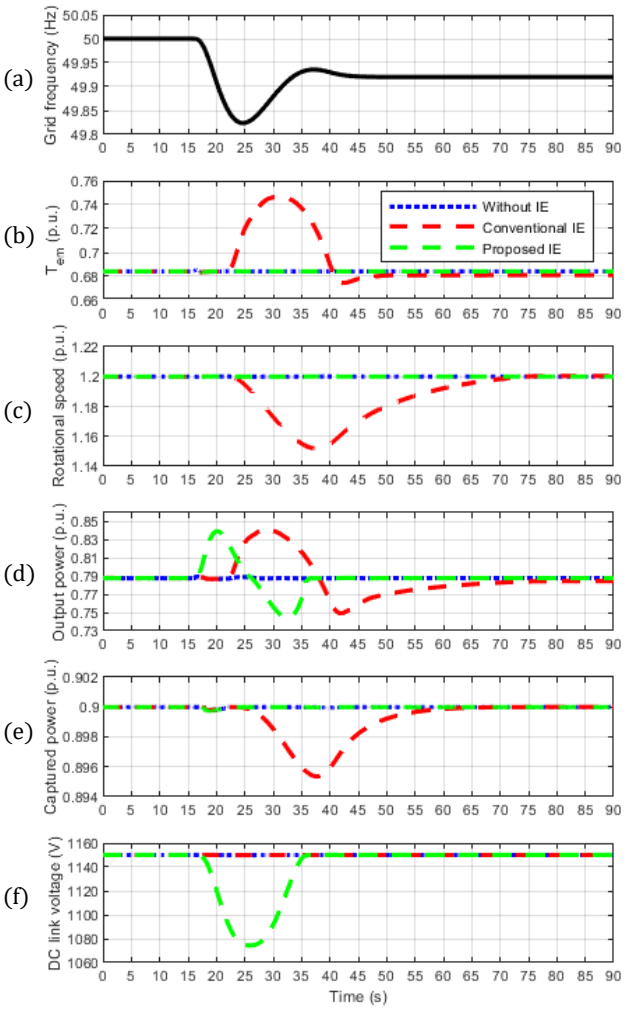

Fig. 4. Simulation results for the DFIG inertial response comparison: (a) grid frequency (Hz); (b) T_{em} (p.u.); (c) WT rotational speed (p.u.); (d) WT output power (p.u.); (e) Captured power by the WT rotor (p.u.); (f) Back-to-back converter DC link voltage (V).

Fig. 4(b) shows that, with the DFIG in its standard configuration (Without IE), T_{em} initially experiences a slight increase in response to the reduction in grid frequency. This slight increase in T_{em} tends to decelerate the machine, as T_m remains constant. The controller $G_\Omega(s)$ immediately reacts to this deceleration by decreasing T^*_{em}. The RSC forces T_{em} to follow T^*_{em}. T_{em} rapidly returns to its original value. Due to the immediate response of $G_\Omega(s)$, Ω variation associated with this T_{em} transient is minimal. This minor Ω variation is not even perceived in Fig. 4(c), but its effect is seen in Fig. 4(e), where the WT is not able to capture the maximum available wind power as it has been forced to leave the MPP. Since the WT immediately re-operates in the MPP, the captured energy loss is minimal. As $G_\Omega(s)$ practically does not allow the release of kinetic energy stored in the rotating masses of the WT, the increase in output power is almost insignificant, as shown in Fig. 4(d). Fig. 4(f) illustrates that DC link voltage remains constant at its nominal value (1150V).

With the conventional IE strategy, once the frequency leaves the $Deadband_{\Delta f}$ range, the IE controller reacts by adding ΔT^*_{em}. T_{em} follows its setpoint, as shown in Fig. 4(b). T_{em} is greater than T_m for 18 s. During this time interval, the WT is decelerated due to the torque imbalance (Fig. 4(c)). To allow such Ω variation, $G_\Omega(s)$ response speed has been reduced. The released kinetic energy is injected into the grid, so the WT outputs an additional amount of power during those 18 s (Fig. 4(d)). Maximum turbine output power is

0.84 p.u., which corresponds to an extra amount of 5% of rated power. After these 18 s, $G_{\Omega(s)}$ reacts to the Ω deviation and tries to recover original speed (1.2 p.u.) by providing a T^*_{em} lower than T_m (Fig. 4(b)). The WT accelerates due to the torque imbalance (Fig. 4(c)), so recovery period has started and has a time duration of 35 s. A greater $G_{\Omega(s)}$ response speed would reduce recovery duration. During the recovery, WT output power is lower than the injected power into the grid before the frequency event since a fraction of captured power is spent on accelerating the machine (Fig. 4(d)). Fig. 4(e) illustrates that, from the moment the IE controller reacts to the frequency event until the recovery ends, the machine operates outside the MPP, which means that the captured power is not optimal. Fig. 4(f) shows how the DC link voltage remains constant at 1150V.

With the proposed IE strategy, Fig. 4(b) illustrates that T_{em} responds exactly as in the case of having no IE strategy implemented, since T^*_{em} is not used as a control variable to achieve the IR. Therefore, the rotating speed (Fig. 4(c)) and the captured power (Fig. 4(e)) also evolve identically. As $Deadband_{DC}$ has not been included for this simulation, the IE controller reduces V^*_{DC} from the start of the frequency event. The GSC forces V_{DC} to follow V^*_{DC}, as shown in Fig. 4(f). V_{DC} decreases for 9 seconds until maximum frequency deviation from 50 Hz is reached (frequency Nadir). During this time interval, the released electrical energy from the SC is injected into the grid, so the WT outputs an additional amount of power (Fig. 4(d)). After frequency Nadir, Fig. 4(d) shows that output power is lower than the injected power into the grid before the frequency event since a fraction of captured power is spent on charging the SC (recovery period). Recovery lasts till V_{DC} reaches 1150V, 9 s in this case (Fig. 4(f)). Compared to conventional IE, a recovery period of shorter duration is achieved.

VI. Conclusions

This contribution analyses the IR of WTs to frequency events. Any WT topology will exhibit an IR if T_{em} is sensitive to frequency variations. The IR of a PMSG is null because the DC link included in the back-to-back converter (which provides the only path between generator's stator and the grid) completely decouples T_{em} from grid frequency. In contrast, in a DFIG, T_{em} is sensitive to frequency variations, as the generator's stator is directly connected to the grid. However, the implemented MPPT greatly limits the magnitude and duration of the IR, forcing it to be almost insignificant.

Several TSOs require WPPs to emulate inertia in order to increase wind power penetration without worsening power system's frequency response. The most common technique implemented in WTs for IE relies on pitch control and stored kinetic energy variations. The IE strategy proposed in this contribution (valid for both PMSG and DFIG) achieves a change in output power by varying the charge of a SC connected to the back-to-back converter DC link.

The proposed strategy has been validated by means of simulations carried out in MATLAB/SIMULINK using a 1.6-MW DFIG model, and presents important advantages over ordinary strategy: WT captures the maximum available wind power during the frequency event; it has entire capacity to emulate inertia regardless wind speed conditions; there is no need to limit the IR for low Ω to provide a margin above aerodynamic stall; it is not necessary to restrict the rate of change of output power to alleviate mechanical stresses on the drive train; it avoids the SFD; the frequency recovery to original value is not delayed since it does not overload the primary regulation service; the WT immediately responds to a frequency event due to the SC fast dynamics; the proposed strategy has a higher energy efficiency.

References

[1] J. Machowski, J. W. Bialek, and J. R. Bumby, "Power System Dynamics. Stability and Control," 2012.

[2] A. Mullane and M. O'Malley, "The inertial response of induction-machine-based wind turbines," *IEEE Trans. Power Syst.*, vol. 20, no. 3, pp. 1496–1503, 2005, doi: 10.1109/TPWRS.2005.852081.

[3] A. Mullane, G. Bryans, and M. O'Malley, "Kinetic energy and frequency response comparison for renewable generation systems," in *2005 International Conference on Future Power Systems*, 2005, pp. 6 pp. – 6, doi: 10.1109/FPS.2005.204252.

[4] EirGrid, "Rate of Change of Frequency (ROCOF) Workstream," November, pp. 1–7, 2011.

[5] F. Gonzalez-Longatt, "Impact of synthetic inertia from wind power on the protection/control schemes of future power systems: Simulation study," *IET Conf. Publ.*, vol. 2012, no. 593 CP, 2012, doi: 10.1049/cp.2012.0030.

[6] Z. Wu *et al.*, "State-of-the-art review on frequency response of wind power plants in power systems," *J. Mod. Power Syst. Clean Energy*, vol. 6, no. 1, pp. 1–16, 2018, doi: 10.1007/s40565-017-0315-y.

[7] G. Abad, J. Lopez, M. A. Rodriguez, L. Marroyo, and G. Iwanski, "Doubly Fed Induction Machine: Modeling and Control for Wind Energy Generation," 2011.

[8] A. Sachan, A. K. Gupta, and P. Samuel, "A review of MPPT algorithms employed in wind energy conversion systems," *J. Green Eng.*, vol.6, no. 4,pp. 385–402, 2017,doi:10.13052/jge1904-4720.643.

[9] N. W. Miller and J. J. Sanchez-gasca, "Modeling of GE Wind Turbine-Generators for Grid Studies," 2010.

[10] N. W. Miller, K. Clark, and M. Shao, "Frequency responsive wind plant controls: Impacts on grid performance," *IEEE Power Energy Soc. Gen. Meet.*, pp. 1–8, 2011, doi: 10.1109/PES.2011.6039137.

[11] X. Yan and X. Sun, "Inertia and droop frequency control strategy of doubly-fed induction generator based on rotor kinetic energy and supercapacitor," *Energies*, vol. 13, no. 14, 2020, doi: 10.3390/en13143697.

[12] N. B. Hargreaves, S. M. Pantea, and G. A. Taylor, "Large Scale Renewable Power Generation," 2014.

[13] J. Van De Vyver, J. D. M. De Kooning, B. Meersman, L. Vandevelde, and T. L. Vandoorn, "Droop Control as an Alternative Inertial Response Strategy for the Synthetic Inertia on Wind Turbines," *IEEE Trans. Power Syst.*, vol. 31, no. 2, pp. 1129–1138, 2016, doi: 10.1109/TPWRS.2015.2417758.

[14] J. Licari, J. Ekanayake, and I. Moore, "Inertia response from full-power converter-based permanent magnet wind generators," *J. Mod. Power Syst. Clean Energy*, vol. 1, no. 1, pp. 26–33, 2013, doi: 10.1007/s40565-013-0002-6.

[15] L. Xiong, Y. Li, Y. Zhu, P. Yang, and Z. Xu, "Coordinated control schemes of super-capacitor and kinetic energy of DFIG for system frequency support," *Energies*, vol. 11, no. 1, 2018, doi: 10.3390/en11010103.

[16] M. F. M. Arani and E. F. El-Saadany, "Implementing virtual inertia in DFIG-based wind power generation," *IEEE Trans. Power Syst.*, vol. 28, no. 2, pp. 1373–1384, 2013, doi: 10.1109/TPWRS.2012.2207972.

[17] S. G. Kim and M. Bollen, "Elforsk rapport 13:03," 2013.

[18] A. Berrueta, A. Ursúa, I. S. Martín, A. Eftekhari, and P. Sanchis, "Supercapacitors: Electrical Characteristics, Modeling, Applications, and Future Trends," *IEEE Access*, vol. 7, pp. 50869–50896, 2019, doi: 10.1109/ACCESS.2019.2908558.

[19] ENTSO-E, "Inertia and Rate of Change of Frequency (RoCoF)," *Exec. Summ.*, 2020, [Online]. Available: https://eepublicdownloads.azureedge.net/clean-documents/SOC documents/Inertia and RoCoF_v17_clean.pdf (accessed Jul. 26, 2021).

[20] R. Gagnon, "Wind Farm - DFIG Detailed Model Matlab Simulink," *Mathworks-Simulink*. [Online]. Available: https://es.mathworks.com/help/physmod/sps/ug/wind-farm-dfig-detailed-model.html (accessed Jul. 26, 2021).

[21] M. Fischer, S. Engelken, N. Mihov, and A. Mendonca, "Operational experiences with inertial response provided by type 4 wind turbines," *IET Renew. Power Gener.*, vol. 10, no. 1, pp. 17–24, 2016, doi: 10.1049/iet-rpg.2015.0137.